



1 Diversity, distribution and nitrogen use strategies of bacteria in the South China Sea basin

2

3 Yuan-Yuan Li¹, Xiao-Huang Chen¹, Peng-Fei Wu¹, Dong-Xu Li¹, Lin Lin¹, Da-Zhi Wang^{1,2*}

4

5 ¹State Key Laboratory of Marine Environmental Science/College of the Environment and Ecology, Xiamen

6 University, Xiamen, 361005, China

7 ²Key Laboratory of Marine Ecology & Environmental Sciences, China Academy of Sciences, Qingdao,

8 266071, China

9

10 **Correspondence:** Da-Zhi Wang (dzwang@xmu.edu.cn)

11

12

13

14

15

16

17

18

19

20

21

22

23

24

25

26

27

28



29 **Abstract** The diversity and abundance of bacteria and diazotrophs in the euphotic and aphotic layers of the
30 South China Sea (SCS) basin were investigated based on high-throughput sequencing of the 16S rRNA and
31 nifH genes. Bacterial communities in the aphotic layers significantly differed from those at the euphotic
32 layers, and were characterized by geographical specificities. *Prochlorococcus* and *Alphaproteobacteria* were
33 abundant in the surface layer, whereas *Gammaproteobacteria* was more common in the aphotic layers.
34 *Moraxellaceae* was the most abundant group in the aphotic layer in the northern basin of the SCS (nSCS),
35 while *SAR324*, *SAR202* and *SAR406* occurred mainly in the southern basin of the SCS (sSCS). Diazotrophic
36 *Alphaproteobacteria* was the predominant group in the SCS basin, whereas Marine Group II *Euryarchaeota*
37 emerged in the euphotic bottom of both nSCS and sSCS. Abundances of genes encoding amino acid
38 transporters and ammonium assimilating enzymes were relatively high in the SCS surface and the entire
39 water column of the sSCS, while expression levels of urea and ammonium transporter-encoding genes were
40 the highest at the surface of the SEATS site. Iron deficiency-induced gene *IdiA* and urease were highly
41 expressed at the A2 site. Our results indicated that bacterial communities in the SCS were depth-stratified
42 and exhibited geographic divergency in the aphotic layers between nSCS and sSCS. Amino acids and
43 ammonium were the major nitrogen sources for bacteria while urea, ammonia and nitrite played important
44 roles in regulating cell growth of *Prochlorococcus* in different regions of the SCS.

45

46

47

48

49

50

51

52

53

54

55

56



57 **1 Introduction**

58 As a key component of the marine ecosystem, bacteria play indispensable roles in the carbon cycling and
59 regulation of global climate (Pedro \acute{s} -Alio \acute{c} , 2006). The diversity and distribution of bacterial communities in
60 the oceans are influenced by various environmental factors (DeLong et al. 2006; Daryabor et al. 2016).
61 Nitrogen (N), an essential macronutrient for bacteria, is one of the most important factors regulating
62 bacterial growth, diversity and distribution in the oceans, especially in the subtropical and tropical
63 oligotrophic oceans, in which dissolved inorganic N is almost undetectable. Accordingly, bacteria have
64 evolved diverse strategies to adapt to ambient N deficiency, i.e. up-regulating expressions of high-affinity
65 transporters or utilizing dissolved organic N (DON), such as urea, amino acids and polyamines (Kent et al.,
66 2016). In addition, N fixation by diazotrophs represents another important adaptive strategy for bacteria to
67 survive in N-deficient environments (Montoya et al., 2004). Unicellular and filamentous diazotrophs are
68 found in the oligotrophic oceans and contribute significantly to N cycling in the global oceans. Therefore,
69 the elucidation of N utilization strategies of bacteria will advance our understanding of the diversity and
70 distribution of bacteria in different oceanic regions.

71 The South China Sea (SCS) is one of the largest marginal seas in the world, characterized by permanently
72 stratified and oligotrophic waters. N is nearly undetectable in surface waters, and the N deficiency severely
73 limits bacterial growth and productivity (Wu et al. 2003). Metagenomics of the water column in the South
74 East Asia Time-series Study (SEATS) site reveals that *Alphaproteobacteria* dominate the surface bacterial
75 community while *Gammaproteobacteria* thrive in the deep waters (Tseng et al. 2015). *Prochlorococcus* is
76 the most prevalent autotrophic picoplankton, occurring particularly in summer (Liu et al. 2007; Xie et al.
77 2018). *SAR11* represents the predominant species in all regions and *Cyanobacteria* proliferate mainly in the
78 euphotic layer of the north SCS (Jiang et al., 2013). To date, the explorations on N-fixing bacteria in the SCS
79 basin are still in progress. Using quantitative PCR and molecular cloning methods, *Alphaproteobacteria* and
80 *Gammaproteobacteria* have been identified as the main diazotrophs in the euphotic zone of the SCS basin,
81 while *Trichodesmium* and unicellular *Cyanobacteria* exhibit very low abundances (Zhang et al., 2011).
82 *Gammaproteobacteria* and *Richelia* dominate the diazotrophic communities in the Vietnam Bay and the
83 Mekong river, respectively (Moisander et al., 2008; Bombar et al., 2011). A pyrosequencing study targeting
84 the *nifH* gene reveals that *Gammaproteobacteria* and *Trichodesmium* are the two dominant *nifH*



85 phylogenetic groups in the nSCS (Xiao et al. 2015). These studies have substantially improved our
86 understanding of the bacterial diversities in the SCS basin. Nevertheless, most of them are conducted in the
87 nSCS and the coast regions of the sSCS, while almost no effort has been devoted to the sSCS basin.
88 Moreover, previous studies fail to identify key or new unicellular diazotroph species due to the limitations of
89 methodologies.

90 Isotopic tracing, quantitative PCR and meta-omic approaches have been applied to study the marine N cycle
91 in the SCS and to provide instructive information. *Proteobacteria*, *Cytophaga-Flavobacteria* and
92 *Cyanobacteria* have been demonstrated to play pivotal roles in nitrate assimilation in the nSCS (Cai and Jiao,
93 2008). Bacteria are found to exhibit depth-dependent metabolic potentials, and the metabolism of urea and
94 amino acids is more active at the surface of nSCS (Wang et al., 2010; Tseng et al., 2015). In addition, the
95 nSCS basin shows lower N₂ fixation activity than the East China Sea and the nSCS shelf (Wu et al., 2018).
96 However, systematic studies on N use strategies of bacterial communities in the SCS basin are still scarce.

97 The present study examined the diversity and spatial distributions of bacteria and diazotrophs in the SCS
98 basin using high-throughput sequencing of the 16S rRNA and *nifH* genes. The SEATS site located at the
99 nSCS and the SS1 site located at the sSCS were selected to compare bacterial communities throughout the
100 entire water column, including the surface layer, the deep chlorophyll maximum (DCM) layer, the bottom of
101 the euphotic layer at a depth of 200 m and the oxygen minimum zone (OMZ) at 750 m. PICRUST
102 predictions and real-time qPCR analysis of major N utilization genes were used to infer the N use strategies
103 of bacterial communities. This study provides insights into the diversity and distribution of bacteria and
104 diazotrophs in complex hydrological environments and nitrogen utilization strategy in the marginal basin
105 regions. It also serves as a pioneer study for the comparison of bacterial N utilization strategies between the
106 nSCS and sSCS regions.

107

108 **2 Materials and methods**

109 **2.1 Sample collection and environmental characteristics**

110 Bacterial samples were collected from 5th June to 27th June 2017 during the southwest monsoon prevailing
111 period. The SEATS site (18 °15'N and 115 °30'E) was located at the nSCS, and the other four sites, SS1, A2,
112 B1 and C1, were located at the sSCS (10 °-15 °N and 110 °-120 °E) (**Fig. 1; Table 1**). Seawater at 5 m depth



113 from sites A2, B1 and C1, and seawater at four different depths from SEATS and SS1 sites (5, 68, 200 and
114 750 m from SEATS, 5, 105, 200 and 750 m from SS1) were collected using Niskin bottles attached to a
115 CTD rosette. Approximately 10 L seawater was pre-filtered through a 3 μm pore-size polycarbonate
116 membrane (47 mm diameter, Millipore) and then retained on a 0.22 μm pore-size polycarbonate membrane.
117 The membranes were then stored at -80 $^{\circ}\text{C}$ on board until use.

118 Temperature, salinity, depth and dissolved oxygen data were retrieved from the
119 conductivity-temperature-depth rosette system (CTD, Sea Bird Electronics). Water samples for analysis of
120 inorganic nutrients ($\text{NO}_2^- + \text{NO}_3^-$, NO_2^- , SiO_3^{2-} , PO_4^{3-}) were filtered through a 0.22 μm pore-size
121 polycarbonate membrane and then analyzed immediately on board using the automatic continuous AA3 flow
122 analyzer (Germany) (Fei and Sun, 2011). Sea surface temperature and salinity data were obtained using the
123 Seabird SBE21 apparatus. Seawater for chlorophyll a (Chla) determination was filtered on a 0.45 μm
124 pore-size GF/F membrane (Whatman) and then analyzed using the Turner Designs Model 10 fluorometer.

125

126 **2.2 Nucleic acid extraction and reverse transcription**

127 Environmental DNA of each sample was extracted using the FastDNA SPIN Kit (MP Laboratories, Inc.)
128 following the protocol of the manufacturer. Three biological repeats of environmental RNA were extracted
129 using the Trizol reagent and chloroform, followed by purification using the RNeasy Mini Kit (Qiagen,
130 Germany) as described by Atshan et al. (2012). Reverse transcriptional experiment was immediately
131 conducted following the instruction of the QuantiTect Reverse Transcription Kit (Qiagen, Germany). The
132 extracted DNA and synthetic cDNA samples were stored at -20 $^{\circ}\text{C}$.

133

134 **2.3 PCR and sequencing of 16S rRNA and nifH genes**

135 The V3 and V4 regions of 16S rRNA gene in the environmental DNA samples were amplified with
136 region-specific primers 341F (5'-CCTAYGGGRBGCASCAG-3') and 806R
137 (5'-GGACTACNNGGGTACTAAT-3') (Yu et al. 2005). Fragments of the nifH gene in all DNA samples
138 were amplified with specific primers nifH-F (5'-AAAGGYGGWATCG GYAARTCCACCAC-3') and
139 nifH-R (5'-TTGTTSGCSGCR TACATSGCCATCAT-3') as recommended by Tr  k and Kondorosi (1981).
140 Routine PCR was carried out using the following thermal cycle: 95 $^{\circ}\text{C}$ for 3 min, 27 cycles (35 cycles for



141 nifH) of 95 °C for 30 s, 55 °C for 30 s, 72 °C for 45 s, and finally 72 °C for 10 min. The triplicate PCR
142 products from each sample were purified by 2% agarose gel electrophoresis and extracted using the AxyPrep
143 DNA Gel Extraction Kit (Axygen, USA). The purified 16S rRNA amplicons were sequenced using
144 paired-end sequencing (2 × 250) on the MiSeq platform from Illumina, Inc. Raw reads were de-multiplexed,
145 quality-filtered using QIIME (v1.9.1) with the criteria as described by Li et al. (2018). The resulting
146 qualified 16S rRNA sequences were aligned to the Silva database (Release 128, <http://www.arb-silva.de>),
147 while the nifH sequences were aligned to the FunGene database under GeneBank (Release 7.3,
148 <http://fungene.cme.msu.edu/>). Operational taxonomic units (OTUs) were defined with a percentage
149 sequence similarity of $\geq 99\%$ based on the RDP Bayesian classifier algorithm (v2.2). The sequences of
150 16S rRNA and nifH genes were deposited in GenBank under the BioProject ID PRJNA434503. The
151 individual accession numbers were SAMN08563407-08563415 for the 16S rRNA samples and
152 SAMN08563568-08563574 for the nifH samples.

153

154 **2.4 Design and validation of *Prochlorococcus* specific primers**

155 Using the genomes of the sequenced *Prochlorococcus* strains provided by the Cyanobacterial
156 KnowledgeBase (Peter et al. 2015) as templates, eight group-specific primers targeting N utilizing genes,
157 including ammonia transporter (*amt1*), urea transporter (*urtA*), amino acid transporter (*AAT*), nitrite
158 reductase (*nirA*), urease (*ureA*), glutamine synthetase (*GlnA*), ferredoxin-dependent glutamate synthase
159 (*GltS*) and irondeficiency-induced gene (*IdiA*), were designed using the online Primer Designing Tool (PDT)
160 (**Table S1**). Primers targeting *urtA* and *amt1* genes were referenced from a previous study (Li et al. 2018).
161 Cyanobacteria-specific primers (16SCF: 5'-GGCAGCAGTGGGGAATTT TC-3' and 16SUR:
162 5'-GTMTTACCGCGGCTG CTGG-3') were used as internal control genes (Kyoung-Hee et al., 2012) to
163 minimize sampling or processing differences among samples. To ensure the specificity of the primers, only
164 hyper-conserved sequences among different *Prochlorococcus* ecotypes were conveyed to the automatic
165 generation area of PDT. Amplified products for each pair of primers were separated on agarose gel and then
166 cloned into a T-vector (Takara). At least 35 clones were randomly chosen, fully sequenced and aligned to the
167 NCBI database. Only the primers that yielded more than 30 positive clones with identity > 90% and E-value
168 < 0.01 were considered qualified (Bayer et al., 2014; Li et al., 2018).



169 **2.5 Quantitative real-time PCR assay**

170 Levels of gene expression were quantified on an ABI 7500 instrument. The qPCR reaction was performed
171 following the protocol of the SYBR Green PreMix Plus Kit (Qiagen, Germany) in a volume of 20 μ L. 0.4
172 μ L ROX Reference Dye was added to correct the errors of the fluorescent signals between holes. The
173 thermal cycle conditions were set as follows: preheating at 95 $^{\circ}$ C for 15 s, followed by 40 cycles, with each
174 cycle of heating at 95 $^{\circ}$ C for 15 s and 60 $^{\circ}$ C for 1 min. Relative quantification of target genes was performed
175 by the matched 7500 software (v1.3.1) with the baselines and the cycle threshold (Ct) values set
176 automatically. The relative levels of gene expression were calculated using the $2^{-\Delta\Delta CT}$ method as described
177 by Livak and Schmittgen (2001).

178

179 **2.6 Statistical analysis**

180 The within-habitat diversity (α -diversity) was assessed by the Ace and Shannon indices using the Mothur
181 software (v1.30.1) at a cutoff level of 1%. The between-habitat diversity was assessed by the principal
182 coordinates analysis (PCoA) and the hierarchical clustering analysis based on the Bray-Curtis distance
183 calculated with QIIME Pipeline (Caporaso et al. 2010). The unweighted pair-group with arithmetic mean
184 algorithm was used to build the tree structure. Both the correlations between community structures (revealed
185 from Bray-Curtis distance) and environmental factors, and community diversity estimators with
186 environmental factors, were analyzed by the Mantel test in R software (v3.4.3, vegan package). The
187 Spearman's correlation analysis was performed to assess the correlations between species and environmental
188 factors using the IBM Predictive Analytics Software (PASW) Statistics (v18). All generated coefficients
189 were subjected to the t-test for significance analysis. The heatmaps were generated using the R package
190 "pheatmap".

191 Based on the 16S rRNA dataset, PICRUSt (v0.9.2) was used to predict the functional contents of the
192 metagenome. The abundances of OTU at 99% identity were standardized by removing the influence of 16S
193 rRNA marker gene on the genome copy numbers to ensure that the OTU abundances accurately reflected the
194 true abundances of the designated organisms. Each OTU was then mapped to the Greengenes database
195 (v13.5) for functional prediction. The resulting functional predictions were assigned to the EggNOG
196 database (v4.0) for all genes. The free online Majorbio I-Sanger Cloud Platform (www.i-sanger.com) was



197 used for the bioinformatics analysis.

198

199 **3 Results**

200 **3.1 Physicochemical parameters**

201 The upper mixed water layer of the nSCS near the Luzon Strait was obviously affected by the Kuroshio
202 Current, characterized by high temperature (30 to 31 °C) and high salinity (33.5 to 34). The sSCS surface
203 was dominated by high temperature and sub-high salinity (32.5 to 33.5). The concentrations of NO_x and
204 PO₄³⁻ were undetectable in the SCS surface while the concentration of SiO₃²⁻ varied between 1 μM and 7 μM.
205 With increasing water depth, the temperature and concentration of dissolved oxygen decreased rapidly, but
206 the concentrations of nutrients increased (**Table 1**). The concentration of Chl_a ranged from 0.08 mg/m³ to
207 0.25 mg/m³ among the sampling sites. The depth corresponding to maximum Chl_a concentration was around
208 68 m in the SEATS site and 105 m in the SS1 site, and the bottom of the euphotic layer was around 200 m.

209

210 **3.2 Bacterial community diversity and overall 16S rRNA composition**

211 In this study, sequencing of the V3 and V4 hypervariable regions of 16S rRNA gene was performed to
212 characterize the composition and diversity of bacterial communities. Illumina sequencing generated 823,
213 138 reads in total after quality control. On average, 74, 830 reads were generated per sample with a length of
214 435 bp per read. With the 99% similarity criteria, a total of 1, 427 different OTUs were obtained from 11
215 samples with the average OTU number of 582. The coverage for each sample exceeded 99%, indicating that
216 the selected sequences could indeed represent the bacterial communities of individual samples (**Table S2**).

217 The bacterial alpha diversities were evaluated by the Ace and Shannon estimators. Bacterial community
218 richness (Ace) of the surface and DCM layers was lower than that of the deep layers (**Fig. 2A**). On the
219 contrary, the within-habitat diversity (Shannon) of bacterial community decreased with increasing water
220 depth in SEATS but increased in SS1 (**Figure 2C; Table S2**). To examine the differences of bacterial
221 community composition between the habitats, OTU and Bray-Curtis distance-based PCoA plot and
222 hierarchical clustering analysis were further performed. The samples were found to form five major clusters:
223 samples from the surface layers, and samples at 200 m and 750 m within the same site were clustered
224 together, respectively, while the two DCM samples formed a separate cluster. However, the DCM sample



225 from SS1 exhibited high similarity with the surface sample while the DCM sample from SEATS shared high
226 similarity with the deep layer samples from SEATS (**Fig. 2E, G**).

227 Regarding the horizontal distribution of bacterial community, *Cyanobacteria* was predominant in the surface
228 water of the SCS, accounting for 40.1, 56.2, 53.6, 41.7 and 49.6% of the total bacterial community in
229 SEATS, SS1, A2, B1 and C1, respectively (**Fig. 3A**), whereas the sequences originating from
230 *Prochlorococcus* formed the major cluster (**Fig. 4**). *Proteobacteria* was the second most prevalent group,
231 averagely accounting for 34.6% of the surface bacterial community. *Alphaproteobacteria* showed the highest
232 abundance (18.1% to 26.2%), while *Gammaproteobacteria* showed the second highest abundance (7.5% to
233 11.9%), although significantly lower than that of *Alphaproteobacteria* (**Fig. 3E**). The families of
234 *Rhodospirillaceae*, *SAR86*, *OMI* clade and *SAR11* were frequently detected in the surface samples with
235 relative abundances ranging from 4% to 10% (**Fig. 4**).

236 The vertical profiles of bacterial composition of SEATS and SS1 were then investigated (**Table S3**).
237 *Proteobacteria* was the major phylum at deep layers of SEATS, accounting for 66% to 88% of the bacterial
238 community in the 68 m, 200 m and 750 m layers, while *Gammaproteobacteria* was the most abundant class
239 (**Fig. 3B, E**). At the SS1 site, *Cyanobacteria* was relatively abundant (47.3%) in the DCM layer, whereas
240 *Alphaproteobacteria* represented the second largest group. At the 200 m and 750 m layers of SS1 site, the
241 relative abundances of the phyla *Proteobacteria*, *Chloroflexi* and *Marinimicrobia* increased, while
242 *Proteobacteria* dominated the bacterial communities. *Alpha*-, *Gamma*- and *Deltaproteobacteria*, which
243 accounted for similar proportions, were determined as the major lineages (**Fig. 3B, E**).

244 The top ten most abundant OTUs at the family levels in the 16S rRNA sequencing data exhibited regional
245 differences between the SEATS and SS1 sites. *Prochlorococcus* dominated the surface bacterial community,
246 and *Acinetobacter*, with a relative abundance between 29.3% and 61.4%, represented the most abundant
247 OTU throughout the water column of SEATS. However, the compositions of the abundant OTUs varied
248 among water layers. *Flavobacteriaceae*, *Vibrionaceae*, *Prochlorococcus* and *Shewanellaceae* represented
249 over 40% of the bacterial community at the DCM layer of SEATS, but accounted for much smaller
250 percentages in the deep layers. Abundances of *Pseudoalter*, *Halomonadaceae* and *Alteromonadaceae* were
251 found to increase in the oxygen-deficient layer (750 m) of SEATS. *Prochlorococcus* (38.9%) remained as
252 the dominant group in the DCM layer of SS1 site. It is noteworthy that the top five most abundant OTUs in



253 the 200 m and 750 m layers of SS1 site were identical. The five OTUs, which accounted for 6.0% to 18.9%
254 of the communities, were *SAR324*, *SAR406*, *SAR202*, *SAR11* and *Rhodospirillaceae*, (**Fig. 4**).

255 The top ten most abundant depth-dependent OTUs from SEATS and SS1 sites are listed in **Fig. 5**.
256 Cyanobacterial *Prochlorococcus* and *Synechococcus*, and *OM1* clade were mainly present in the euphotic
257 layers, whereas *Alteromonadaceae*, *Halomonadaceae* and *Pseudoalteromonadaceae* existed mainly in the
258 OMZ of SEATS. By aligning the OTUs across all depths of the SS1 site, *Oceanospirillales*, *Salinispha*,
259 *SAR202*, *SAR324* and *SAR406* exhibited prominent depth specificity in the euphotic bottom layer and OMZ.

260

261 **3.3 Diazotrophic community diversity and overall nifH composition**

262 A total of 131, 569 qualified reads were retrieved from ten nifH samples, and were clustered into 749
263 different OTUs using a sequence cutoff value of 1%. On average, the length per read was 418 bp and the
264 unique OTU number per sample was 181 (**Table S4**). Surface samples, except for the samples from the
265 SEATS site, presented significantly higher community richness than the deep water samples, and the DCM
266 samples displayed the lowest community richness (**Fig. 2B**). The within-habitat diversity of diazotrophic
267 communities was highest in the euphotic bottom layer of SEATS, and was also at high levels in the surface
268 samples of A2, B1 and C1 (**Fig. 2D; Table S4**). Samples from the deep layers (68 m to 750 m) of SEATS
269 and the deep layers (105 m and 200 m) of SS1 were independently clustered and clearly separated from the
270 surface samples (**Fig. 2E, H**). Notably, the surface samples shared high similarity with the deep water
271 samples from the SS1 site.

272 In contrast with the bacterial community, *Proteobacteria* was the principal phylum in all samples (40.2% on
273 average) except for the samples from the euphotic bottom layer (200 m) at the SEATS site, where
274 *Proteobacteria* only accounted for 5.5% (**Fig. 3C, D; Table S5**). *Alphaproteobacteria* was the most
275 abundant group in the surface and DCM layers of the SEATS site. *Betaproteobacteria* was more prevalent in
276 the DCM layer (105 m) and the euphotic bottom layer (200 m) at the SS1 site, while its abundance was very
277 low in the samples from SEATS. While *Gammaproteobacteria* represented the most abundant class in the
278 OMZ of SEATS, it was detected in the surface with markedly lower abundance (**Fig. 3F**).

279 *Cyanobacteria* was the dominant phylum in the DCM layer (68 m) of SEATS, accounting for 41.3% of the
280 diazotrophic community. *Euryarchaeota* and *Actinobacteria* were more abundant at the euphotic zone of



281 SEATS (**Fig. 3D**). *Rhodobacteraceae* represented the most abundant OTU at the surface, while
282 *Rhodocyclales* and *Neisseriaceae* were the second abundant OTUs at the surfaces of SEATS and SS1,
283 respectively. Notably, the family of *Neisseriaceae* increased in relative abundance, accounting for more than
284 20% of the entire diazotrophic community in the DCM and euphotic bottom layers from the SS1 site.
285 *Chroococcales* was the dominant family in the DCM layer of SEATS, while the families of
286 *Rhodobacteraceae*, *Synechococcaceae*, *Rhodospirillaceae* and *Comamonadaceae* contributed substantially
287 to the diazotrophic composition with the portions ranging from 5% to 11%. No major N-fixing
288 microorganisms were found in the euphotic bottom layer of the SEATS site, but a subset of *Euryarchaeota*
289 groups emerged. In the 750 m layer, where oxygen was deficient, *Pseudomonadaceae* exhibited remarkable
290 increases in relative abundance and became the major diazotroph (**Fig. 6; Table S5**).

291 Depth specificity of OTUs in the diazotrophic community was identified at each layer in the water column at
292 the SEATS and SS1 sites. *Desulfovibrionaceae*, *Cellvibrionaceae*, *Chromatiaceae* and *Xanthomonadaceae*
293 were only detected in the surface, while *Rhodospirillaceae*, *Rhodospirillales* and *Flavobacteriaceae* were
294 only observed in the DCM layer. *Actinobacteria* and *Euryarchaeota* were mainly distributed in the euphotic
295 bottom layer, whereas *Ardenticatenaceae*, *Burkholderiales* and *Pseudomonadaceae* exhibited prominent
296 depth specificity in the OMZ of the SEATS site (**Fig. 5C, D**).

297

298 **3.4 Abundances and expressions of N-utilization genes in bacterial community**

299 Based on comparison with the EggNOG database, four groups of N-utilizing COGs in the samples were
300 predicted as “Transporter”, “Inorganic N metabolism”, “Urea metabolism” and “N fixation” (**Fig. 7; Table**
301 **S6**). The COGs assigned to ammonium transporters (*AmtB*, COG0004), ammonium assimilation enzymes
302 (*GlnA*, COG0174 and *GltB*, COG0067) and amino acid transporters (*AMT*, COG0004) were the most
303 abundant in the surface, while abundances of COGs assigned to ureases (*UreABCD*,
304 COG0829-COG0832, COG0804, COG0378) and *nifH* (COG1348) were the second most abundant genes in
305 the surface. Insignificant variations and the lowest abundances of nitrate reductase and nitrite reductase
306 (*NirBD*, COG1251 and COG2146) were observed in different surface samples (**Fig. 7A**).

307 The abundances of N-utilizing COGs varied significantly in different water layers of SEATS and SS1 (**Fig.**
308 **7B**). The abundances of COGs attributed to *AMT*, *AAT*, *NirBD*, as well as the two ammonium assimilation



309 enzymes *GlnA* and *GltB*, were relatively high through the water column of SS1, especially in the surface and
310 DCM layers. *NifH* and *UreABCD* were mainly distributed in the surface and DCM layers of SS1.
311 Although the abundance of nitrate reductases was extremely low throughout the water column, the
312 abundances of subunits *NarI* (COG2181) and *NrfA* (COG3303) increased slightly in the 200 m and 750 m
313 layers of SS1. In addition, a large number of unclassified ABC transporters were predicted in each sample.
314 The relative expression levels of *amt1* and *urtA* were the highest at the surface of SEATS (**Fig. 8**). The
315 expression levels of *AAT* and *GlnA* showed insignificant changes in different surface samples, except for the
316 lowest expression level of *AAT* in A2. High expression levels of *IdiA*, *ureC* and *GltS* were observed in the
317 surface layer of A2. In particular, the expression level of *nirA* gene, which is responsible for the assimilation
318 of nitrite in *Prochlorococcus*, was highest at the surface of SS1. High expression levels of *amt1*, *urtA* and
319 *AAT* were observed at the surface of SEATS. Notably, the relative abundance of *urtA* was approximately
320 ten-fold higher than that of *amt1* and *AAT* (**Fig. 8**).

321

322 **3.5 Environmental influence on community diversity and structure**

323 The results of Mantel test and Spearman analysis showed that the temperature, salinity, dissolved oxygen
324 and nutrients exhibited significant correlations with the structures (Bray-Curtis distance) and
325 between-habitat diversities of both bacterial and diazotrophic communities (**Table 2**; **Table S7**). Nutrients
326 were found to exert greater impacts on bacterial communities, as the concentrations of nitrate and phosphate
327 exhibited significant positive correlations with the within-habitat bacterial richness.

328

329 **4 Discussion**

330 **4.1 Spatial distribution of bacteria in the SCS basin**

331 In this study, high similarity in the bacterial composition among surface samples was observed, as indicated
332 by both the PCoA plot and UPGMA dendrogram. *Cyanobacteria* dominated the five surface samples,
333 comprising primarily oligotrophic *Prochlorococcus* representatives. It is well recognized that
334 *Prochlorococcus* is prevalently distributed in the oligotrophic oceans globally, and the distribution pattern
335 may contribute to its low nutrient adaptability (Jing and Liu, 2012; Garcia-Fernandez et al., 2004;
336 Zwirgmaier et al., 2007; Liu et al., 2007). Cai et al. (2007) and Liu et al. (2007) report the seasonal



337 distributions of picoplankton in the nSCS, and show that the abundance of *Prochlorococcus* is higher in
338 summer than in winter, while Xie et al. (2018) demonstrate that *Prochlorococcus* dominates the
339 phytoplankton community in the SCS basin.

340 *Alphaproteobacteria* was more abundant in all surface samples while *Gammaproteobacteria* was more
341 common in the deep layers of SEATS, in agreement with the previous studies based on 16S rRNA
342 sequencing and metagenomic approaches (Jing et al., 2013; Tseng et al., 2015). Furthermore, *Alpha*-,
343 *Gamma*- and *Deltaproteobacteria* contributed equally to the deep layer samples of SS1. These results were
344 consistent with the clustering results, indicating that the bacterial communities in upper waters were
345 separated from their deep-water counterpart, but the deeper-water community also exhibited geographical
346 specificities.

347 Pronounced stratification among specific bacterial groups from the SEATS and SS1 sites was observed, in
348 accordance with previous phylogenetic surveys (DeLong, 2005; Hewson et al., 2006; Treusch et al., 2009;
349 Galand et al. 2010; Kirchman et al., 2010; Agogue et al., 2011). For instance, *SAR324*, *SAR406* and *SAR202*
350 clades were relatively abundant in the euphotic and oxygen-deficient layers of SEATS and SS1. These
351 groups are also reported as typical deep-water clades in the deep Atlantic and Pacific oceans (Wright et al.,
352 1997; Morris et al., 2004; DeLong et al., 2006; Pham et al., 2008; Agogue et al., 2011). *SAR324*-like reads
353 are abundant in the OMZs of the coastal regions in Iquique (Ganesh et al., 2014). Meanwhile, differences in
354 bacterial distributions between SEATS and SS1 were observed. The family *Moraxellaceae*, comprising
355 primarily the genus of *Acinetobacter*, was the most abundant family in the deep layers of SEATS, but was
356 rarely detected in SS1. Jing et al. (2013) report its prevalence in SEATS, although only in the deep-water
357 layer of 2000 m, and Xia et al. (2015) find that *Moraxellaceae* is abundant in the surface water of the SCS,
358 and even higher *Moraxellaceae* abundance was detected in summer. In addition, *Moraxellaceae* also shows
359 high relative abundance in the estuary ecosystem of Zhuhai (Li et al., 2018) and in the sediments of
360 Okinawa Island (Soliman et al., 2017). The family *Moraxellaceae*, commonly found in naturally saline
361 environments, can proliferate under a broad range of temperatures and can remineralize organic matters *in*
362 *situ* (King et al. 1997; Okabe et al. 2003; Teixeira and Merquior, 2014). Nevertheless, little is known about its
363 ecological roles, such as its role in the degradation of organic compounds. Meanwhile, few bacterial groups
364 exhibited preferential distribution at the bottom of the euphotic layer of SEATS, characterized by



365 co-limitation of iron and light (Mitchell et al., 1991; Nelson and Smith, 1991). However, the groups of
366 *Alteromonadaceae*, *Halomonadaceae* and *Pseudoalteromonadaceae* featured depth-specific distributions in
367 the OMZ of SEATS, while were negligible in SS1 as well as other typical OMZ bacterial communities
368 (Ganesh et al., 2014; Hawley et al., 2014). This discrepancy might be attributed to the perturbations brought
369 by Kuroshio intrusion and mesoscale eddies experienced in SEATS, since heterotrophic bacteria, particularly
370 *Oceanospirillales* and *Alteromonadales*, display high abundances in the Kuroshio Current and affected areas
371 of cyclonic eddy (Li et al. 2017; Li et al. 2018).

372

373 **4.2 Diazotrophic distribution in the SCS basin**

374 N₂ fixation provides over 10% of the total carbon production in the SCS (Voss et al., 2006). *Trichodesmium*
375 is considered as the main diazotroph in pelagic oceans (Moisander et al., 2008), but recent studies showed
376 that non-cyanobacterial diazotrophs and unicellular cyanobacteria groups are also present and active (Zhang
377 et al., 2011; Moisander et al., 2014; Li et al., 2018). A prominent feature of the SCS during our sampling
378 period was that diazotrophic *Alphaproteobacteria*, comprising primarily *Rhodobacteraceae*, dominated the
379 SCS surface while the abundance of the unicellular *Cyanobacteria* was negligible, in agreement with Zhang
380 et al. (2010), who report the dominance of *Alphaproteobacteria* and lower abundance of both
381 *Trichodesmium* and heterocystous cyanobacterial diatom symbionts in the SCS deep basin area.

382 Inconsistent with the findings of Zhang et al. (2010), Moisander et al. (2008) and Moisander et al. (2014),
383 *Gammaproteobacteria* was rare in our samples except for the OMZ sample of SEATS. Instead,
384 *Betaproteobacteria* was widely distributed at the SEATS and SS1 sites across all depths. In particular,
385 *Betaproteobacteria*, comprising primarily *Neisseriaceae*, overwhelmingly dominated the diazotrophic
386 communities in the DCM and euphotic bottom layers of SS1. *Betaproteobacteria* is a typical freshwater
387 lineage (Zwart et al., 2002) frequently present in the oceans (Brown et al., 2009; Andersson et al., 2010).
388 Phylogenetic analysis of our study revealed that the proportion of *Betaproteobacteria* in the SCS was much
389 smaller, indicating that the survey area was not affected by offshore freshwater inflows. Nevertheless, a
390 concern is that *nifH*-like sequences related to *Betaproteobacteria* may be present in the PCR reagents (Zehr
391 et al., 2003; Goto et al., 2005). Therefore, the identification of *Betaproteobacteria*-like sequences should be
392 treated with caution.



393 In this study, the stratified distribution of bacterial assemblages in SEATS differed from that in SS1.
394 *Chroococcales* dominated the diazotrophic community of the DCM layer at the SS1 site. This group is also a
395 major diazotroph in Arctic and Indian seawaters (Diez et al., 2012; Bauer et al., 2007). N₂-fixing archaea is
396 confined only to the phylum *Euryarchaeota* (Dos-Santo et al., 2012). The group II *Euryarchaeota* (*MG-II*)
397 emerged at the bottom of the euphotic layer of SEATS, accounting for more than 10% of the bacterial
398 community. *MG-II* is distributed within the euphotic zone of temperate waters and plays pivotal roles in
399 marine N cycling (Haro-Moreno et al., 2017; Qin et al., 2014). The presence of the *MG-II* groups inferred
400 the existence of an *Euryarchaeota*-leading diazotrophic community at the bottom of the euphotic zone of
401 SEATS, and confirmed the ecological significance of marine archaea as a new N contributor in deep oceans.
402 The bottom of the euphotic zone is characterized by specific dissolved organic matters, and further
403 investigation is needed to evaluate it as a potential habitat for *MG-II*.

404

405 **4.3 Environmental influences on bacterial community**

406 The gradient physico-chemical characteristics of the water column, such as the declines in light intensity and
407 temperature, as well as the scarce organic matter availability, have been identified as crucial factors
408 impacting the vertical distribution of bacterial communities (Giovannoni et al., 2005; DeLong et al., 2006).
409 The depth and latitude also represent highly significant explanatory variables for the bacterial populations
410 from different water masses in the North Atlantic Ocean (Agogue et al., 2011). In the present study,
411 remarkable differences in bacterial and diazotrophic compositions were identified for SEATS and SS1
412 located at the northern and southern basin regions of the SCS. Temperature, salinity, dissolved oxygen and
413 nutrient concentrations contributed in synergy to the horizontal and vertical variations of bacterial structures,
414 in agreement with the findings of previous studies that the physico-chemical parameters lead to almost
415 identical results, as the vertical stratification in the Northwestern Mediterranean Sea (Ghiglione et al., 2008)
416 and variations of major phytoplankton groups in the SCS are influenced by temperature, irradiance and
417 nutrient concentrations (Zhang et al., 2014; Xiao et al., 2018). In our study, the bacterial community in the
418 DCM layer of SS1 was highly similar to that of the surface water, likely due to the strong vertical mixing in
419 SS1 induced by the tropical storm Merbok that passed through the sampling area.

420 Both bacterial and diazotrophic communities shared similarities in the deep layers, but were distinct in the



421 upper layers, suggesting that the deep-sea assemblages formed a separate cluster from the surface
422 assemblages as revealed in the North Pacific Ocean (Brown et al., 2009). As indicated by the results of the
423 correlation analysis, the concentrations of nitrate and phosphate were the key factors affecting the richness
424 and diversity of bacterial community. Depletion of nutrients, particularly phosphate, in the upper waters
425 contributed to the low richness and diversity of bacterial communities.

426

427 **4.4 N use strategies of bacterial community in the SCS**

428 PICRUSt prediction and real-time qPCR are valuable tools to assess gene expressions in microorganisms
429 from the natural environments (Langille et al., 2013; Li et al., 2018). In epipelagic waters of the SCS, N is
430 one of the limiting nutrients, in contrast to the dark, energy-limited but relatively N-rich deep oceans (Batut
431 et al., 2014; Giovannoni and Nemergut, 2014). The dominant group, *Prochlorococcus*, plays critical roles in
432 marine N cycle of the SCS. To investigate the expressions of N-utilization-related genes in the bacterial
433 communities and *Prochlorococcus* in different regions of the SCS basin, we examined both the gene
434 abundances and expression levels of transporters and N utilization pathways for both the inorganic and
435 organic N sources. Although *IdiA* is not directly involved in the N utilization, the expression of *IdiA* was
436 also taken into account in our study, as iron is essential for nitrite assimilation and N fixation in the cells.

437 The results of PICRUSt prediction and qPCR analysis revealed that the amino acid transporters and
438 ammonium assimilating enzymes were prevalent in the surface of SCS, indicating that the amino acids
439 represent a major N source for the bacterial community, consistent with the results of Zubkov et al. (2003)
440 and García-Fernández et al. (2004). As reported previously, multiple protein biomarkers from
441 *Prochlorococcus* provide indications of nutritional stress, for instance, the urea transporter for nitrogen and
442 *IdiA* for iron (Saito et al., 2014). The expression of urease complex is also up-regulated under N deprivation
443 (Tolonen et al., 2006). Although urea transporter expression was not predicted by PICRUSt, highest
444 expression levels of ureases and ammonium transporters were detected in the surface waters. Consistently,
445 expression levels of urea transporters and ammonium transporters were also relatively high in the surface
446 layer of SEATS, while *IdiA* and urease exhibited the highest expression levels in A2, suggesting N
447 deficiency in SEATS and deficiencies of both iron and N in A2. Ammonium, urea and amino acids were the
448 major N sources for the bacterial community in SEATS, while urea was the major N source in A2. Since iron



449 is an indispensable metal coenzyme for nitrate/nitrite reductase and nitrogenase, it is speculated that
450 nitrate/nitrite reduction and N_2 fixation are limited by iron deficiency, which in turn promotes urea
451 utilization in the cells. In the equatorial Pacific, both urea transporters and *IdiA* from *Prochlorococcus* are
452 among the most abundant proteins, while the urease and urea transporter operons are present at high
453 abundances in the *Prochlorococcus* clades from iron-depleted oceanic regions of the Eastern Equatorial
454 Pacific and Indian Ocean, implying that the dissolved organic N is an important nutritional source for
455 *Prochlorococcus* in the iron-limited regions (Rusch et al., 2010; Saito et al., 2014).

456 Although most phytoplankton species can use ammonia, nitrite and nitrate as sole nitrogen sources, nearly
457 all *Prochlorococcus* isolates use ammonia as their N source except for two low light-adapted
458 *Prochlorococcus* clades (eNATL and eMIT9313), which can also assimilate nitrite (Moore et al., 2002;
459 Martiny et al., 2009). The availability of nitrite may therefore influence the distribution of these two clades,
460 although relevant evidences have not been reported in the field (Bouman et al., 2006; Johnson et al., 2006).
461 In our study, the abundances of *nitrate/nitrite reductases* were extremely low throughout the entire water
462 column of the SCS, even in the nitrate-rich deeper waters, indicating that NO_x -N was not the main N source
463 for the bacterial communities of the SCS basin. However, the qPCR results revealed that the expression
464 level of nitrite reductase was exclusively high in the surface layer of SS1, indicating that a different N
465 utilization strategy with an emphasis on nitrite might exist within SS1 and other sites.

466

467 **4.5 Conclusion and recommendations**

468 Similar horizontal distribution patterns of both bacterial and diazotrophic compositions were observed in the
469 surface of the SCS basin, while different N utilization strategies were found to exist in the bacterial
470 communities and *Prochlorococcus*. Moreover, the bacterial communities and N utilization strategies varied
471 among the typical water masses under the influences of physical and hydrochemical conditions along the
472 water column. Meanwhile, different prevalent OTUs were identified at different depths among the regions of
473 nSCS and sSCS, under the influence of the Kuroshio intrusion into the nSCS basin. The depth was found to
474 be a highly significant explanatory variable for the bacterial populations from different water masses. Given
475 the high spatial heterogeneity inherent to marine environments and the consequent variations of bacterial
476 community structures, a comprehensive study, such as metagenomics and metaproteomics, not only could



477 provide exhaustive characterization of bacterial assemblages, but also would aid the identification of specific
478 bacterial groups and metabolic pathways, thus revealing the specific ecological roles of marine bacterial
479 communities (Venter et al., 2004; DeLong et al., 2006).

480

481 *Data availability.* Data are available in GenBank under BioProjectID PRJNA509084. The individual accession
482 numbers SAMN10537119-10537129 represented 16S rRNA libraries and SAMN10537130-10537139 represented
483 nifH libraries.

484

485 *Author contributions.* WDZ and LYY conceived and designed this study. LYY, WPF and LDX conducted the field
486 work. LYY and CXH analyzed the data. LL contributed to the instrumental analysis. LYY and CXH drafted the paper,
487 and WDZ revised and finalized the paper.

488

489 *Competing interests.* The authors declare that they have no conflict of interest.

490

491 *Acknowledgements.*

492 This study was supported by the National Natural Science Foundation of China through grant 41425021, and
493 the Ministry of Science and Technology through grant 2015CB954003. D.-Z. Wang was also supported by
494 the ‘Ten Thousand Talents Program’ for leading talents in science and technological innovation.

495

496 **References**

497

498 Agogué H., Lamy, D., Neal, P. R., Sogin, M. L., and Herndl, G. J.: Water mass specificity of bacterial
499 communities in the North Atlantic revealed by massively parallel sequencing, *Mol. Ecol.*, 20, 258-274,
500 <https://doi.org/10.1111/j.1365-294X.2010.04932.x>, 2011.

501 Andersson, A. F., Riemann, L., and Bertilsson, S.: Pyrosequencing reveals contrasting seasonal dynamics of
502 taxa within Baltic Sea bacterioplankton communities. *ISME J.*, 4, 171-181, <https://doi.org/10.1038/ismej.2009.108>, 2010.

504 Atshan, S. S., Shamsudin, M. N., Lung, L. T., Ling, K. H., Sekawi, Z., Pei, C.P., and Ghaznavi-Rad, E.:
505 Improved method for the isolation of RNA from bacteriarefractory to disruption, including *S. aureus*
506 producing biofilm. *Gene*, 494,219-224, <https://doi.org/10.1016/j.gene.2011.12.010>, 2012.

507 Batut, B., Knibbe, C., Marais, G., and Daubin, V.: Reductive genome evolution at both ends of the bacterial
508 population size spectrum. *Nat. Rev. Microbiol.* 12, 841-850, <https://doi.org/10.1038/nrmicro3331>, 2014.



- 509 Bauer, K., Diez, B., Lugomela, C., Seppala, S., Borg, A. G., and Bergman, B.: Variability in benthic
510 diazotrophy and cyanobacterial diversity in a tropical intertidal lagoon. *FEMS Microbiol. Ecol.*,
511 63,205-211, <https://doi.org/10.1111/j.1574-6941.2007.00423.x>, 2008.
- 512 Bayer, K., Kamke, J., and Hentschel, U.: Quantification of bacterial and archaeal symbionts in high and low
513 microbial abundance sponges using real time PCR. *FEMS Microbiol. Ecol.*, 89,
514 679-690, <https://doi.org/10.1111/1574-6941.12369>, 2014.
- 515 Bouman, H. A., Ulloa, O., Scanlan, D. J., Zwirgmaier, K., Li, W. K., Platt, T., Stuart, V., Barlow, R., Leth,
516 O., Clementson, L., Lutz, V., Fukasawa, M., Watanabe, S., and Sathyendranath, S.: Oceanographic basis
517 of the global surface distribution of *Prochlorococcus* ecotypes. *Science*, 312, 918-921,
518 <https://doi.org/10.1126/science.1122692>, 2006.
- 519 Brown, M. V., Philip, G. K., Bunge, J. A., Smith, M. C., Bissett, A., Lauro, F. M., Fuhrman, J. A., and
520 Donachie, S. P.: Microbial community structure in the North Pacific Ocean. *ISME J.* 3, 1374-1386,
521 <https://doi.org/10.1038/ismej.2009.86>, 2009.
- 522 Cai, H. Y. and Jiao, N. Z.: Diversity and abundance of nitrate assimilation genes in the Northern South
523 China Sea. *Microb. Ecol.*, 56, 751-764, <https://doi.org/10.1007/s00248-008-9394-7>, 2008.
- 524 Cai, Y. M., Ning, X. R., Liu, C. G., and Hao, Q.: Distribution pattern of photosynthetic picoplankton and
525 heterotrophic bacteria in the Northern South China Sea. *J.Integr. Plant Biol.*, 49, 282-298,
526 <https://doi.org/10.1111/j.1744-7909.2007.00347.x>, 2007.
- 527 Caporaso, J. G., Kuczynski, J., Stombaugh, J., Bittinger, K., and Bushman, F. D., Costello, E. K., Fierer, N.,
528 Peña, A. G., Goodrich, J. K., Gordon, J. I., Huttley, G. A., Kelley, S. T., Knights, D., Koenig, J. E., Ley, R.
529 E., Lozupone, C. A., McDonald, D., Muegge, B. D., Pirrung, M., Reeder, J., Sevinsky, J. R., Turnbaugh, P.
530 J., Walters, W. A., Widmann, J., Yatsunencko, T., Zaneveld, J., and Knight, R.: QIIME allows analysis of
531 high-throughput community sequencing data. *Nat. Methods.*, 7, 335-336,
532 <https://doi.org/10.1038/nmeth.f.303>, 2010.
- 533 Daryabor, F., Ooi, S. H., Samah, A. A., and Akbari, A.: Dynamics of the water circulations in the Southern
534 South China Sea and its seasonal transports. *PLoS ONE*, 11, e0158415,
535 <https://doi.org/10.1371/journal.pone.0158415>, 2016.
- 536 DeLong, E. F., Preston, C. M., Mincer, T., Rich, V., Hallam, S. J., Frigaard, N. U., Martinez, A., Sullivan, M.
537 B., Edwards, R., Brito, B. R., Chisholm, S. W., and Karl, D. M.: Community genomics among stratified
538 microbial assemblages in the ocean's interior. *Science*, 311, 496-503,
539 <https://doi.org/10.1126/science.1120250>, 2006.
- 540 Diez, B., Bergman, B., Pedros-Alio, C., Anto, M., and Snoeijs, P.: High cyanobacterial *nifH* gene diversity
541 in Arctic seawater and sea ice brine. *Environ. Microbiol. Rep.*, 4, 360-366,



- 542 <https://doi.org/10.1111/j.1758-2229.2012.00343.x>, 2012.
- 543 Dos Santos, P. C., Fang, Z., Mason, S. W., Setubal, J. C., and Dixon, R.: Distribution of nitrogen fixation
544 and nitrogenase-like sequences amongst microbial genomes. *BMC Genomics*, 13, 162,
545 <https://doi.org/10.1186/1471-2164-13-162>, 2012.
- 546 Fei, S. D., and Sun, Y. L.: Application of Ultrasonic-continuous Flow Analysis in Waster Water
547 Multi-parameters Detecting [J]; *Guangdong Chemical Industry* 6, 2011.
- 548 Gallagher, J. M., Carton, M. W., Eardly, D. F., and Patching, J. W.: Spatio-temporal variability and diversity
549 of water column prokaryotic communities in the eastern North Atlantic. *FEMS Microb. Ecol.*, 47,249-262,
550 [https://doi.org/10.1016/S0168-6496\(03\)00281-2](https://doi.org/10.1016/S0168-6496(03)00281-2), 2004.
- 551 Ganesh, S., Parris, D. J., DeLong, E. F., and Stewart, F. J.: Metagenomic analysis of size-fractionated
552 picoplankton in a marine oxygen minimum zone. *ISME J.*, 8, 187-211, <https://doi.org/10.1038/ismej.2013.144>, 2014.
- 554 Garcia-Fernandez, J. M., de Marsac, N. T., and Diez, J.: Streamlined regulation and gene loss as adaptive
555 mechanisms in *Prochlorococcus* for optimized nitrogen utilization in oligotrophic environments.
556 *Microbiol. Mol. Biol. Rev.*, 68, 630-638, <https://doi.org/10.1128/MMBR.68.4.630-638.2004>, 2004.
- 557 Ghiglione, J. F., Palacios, C., Marty, J. C., Mevel, G., Labrune, C., Conan, P., Pujo-Pay, M., Garcia, N., and
558 Goutx, M.: Role of environmental factors for the vertical distribution (0–1000 m) of marine bacterial
559 communities in the NW Mediterranean Sea. *Biogeosciences*, 5, 1751-1764,
560 <https://hal.archives-ouvertes.fr/hal-00330300>, 2008.
- 561 Giovannoni, S. J., and Stingl, U.: Molecular diversity and ecology of microbial plankton. *Nature*, 437,
562 343-348, <https://doi.org/10.1038/nature04158>, 2005.
- 563 Giovannoni, S., and Nemergut, D.: Ecology. Microbes ride the current. *Science*, 345, 1246-1247,
564 <https://doi.org/10.1126/science.1259467>, 2014.
- 565 Goto, M., Ando, S., Hachisuka, Y., and Yoneyama, T.: Contamination of diverse *nifH* and *nifH*-like DNA
566 into commercial PCR primers. *FEMS Microbiol. Lett.*, 246, 33-38, <https://doi.org/10.1016/j.femsle.2005.03.042>, 2005.
- 568 Haro-Moreno, J. M., Rodriguez-Valera, F., López-García, P., Moreira, D., and Martin-Cuadrado, A. B.: New
569 insights into marine group III Euryarchaeota, from dark to light. *ISME J.*, 11,
570 1102-1117, <https://doi.org/10.1038/ismej.2016.188>, 2017.
- 571 Hawley, A. K., Brewer, H. M., Norbeck, A. D., Paša-Tolić, L., and Hallam, S. J.: Metaproteomics reveals
572 differential modes of metabolic coupling among ubiquitous oxygen minimum zone microbes. *Proc. Natl.*
573 *Acad. Sci. USA*, 111, 11395-11400, <https://doi.org/10.1073/pnas.1322132111>, 2014.
- 574 Jing, H. M., and Liu, H. B.: Phylogenetic composition of *Prochlorococcus* and *Synechococcus* in cold eddies



- 575 of the South China Sea. *Aquat. Microb. Ecol.*, 65, 207-219, <https://doi.org/10.3354/ame01546>, 2012.
- 576 Jing, H. M., Xia, X. M., Suzuki, K. J., and Liu, H. B.: Vertical profiles of bacteria in the tropical and
577 subarctic oceans revealed by pyrosequencing. *PLOS ONE*, 8, e79423,
578 <https://doi.org/10.1371/journal.pone.0079423>, 2013.
- 579 Johnson, Z. I., Zinser, E. R., Coe, A., McNulty, N. P., Woodward, E. M., and Chisholm, S. W.: Niche
580 partitioning among *Prochlorococcus* ecotypes along ocean-scale environmental gradients. *Science*, 311,
581 1737-1740, <https://doi.org/10.1126/science.1118052>, 2006.
- 582 King, J. E., Jaouhari, R., and Quinn, J. P.: The role of sulfoacetaldehydesulfo-lyase in the mineralization of
583 isethionate by an environmental *Acinetobacter* isolate. *Microbiology*, 143,
584 2339-2343, <https://doi.org/10.1099/00221287-143-7-2339>, 1997.
- 585 Kyoung-Hee, O., Jeong, D. H., Shin, S. H., and Cho, Y. C.: Simultaneous quantification of *Cyanobacteria*
586 and *Microcystis* spp. using real-time PCR. *J. Microbiol. Biotechnol.*, 22,
587 248-255, <http://doi.org/JMB022-02-16>, 2012.
- 588 Langille, M. G., Zaneveld, J., Caporaso, J. G., McDonald, D., Knights, D., Reyes, J. A., Clemente, J. C.,
589 Burkepille, D. E., Thurber, R. L. V., Knight, R., Beiko, R. G., and Huttenhower, C.: Predictive functional
590 profiling of microbial communities using 16S rRNA marker gene sequences. *Nat. biotechnol.*, 31,
591 814-821, <https://doi.org/10.1038/nbt.2676>, 2013.
- 592 Li, J. L., Salam, N., Wang, P. D., Chen, L. X., Jiao, J. Y., Li, X., Xian, W. D., Han, M. X., Fang, B. Z., Mou,
593 X. Z., Li, W. J.: Discordance between resident and active bacterioplankton in free-living and
594 particle-associated communities in estuary ecosystem. *Microb. Ecol.*, 76, 637-647,
595 <https://doi.org/10.1007/s00248-018-1174-4>, 2018.
- 596 Li, Y. Y., Chen, X. H., Xie, Z. X., Li, D. X., Wu, P. F., Kong, L. F., Lin, L., Wang, D. Z.: Bacterial diversity
597 and nitrogen utilization strategies in the upper layer of the Northwestern Pacific Ocean. *Front. Microbiol.*,
598 9, 797. <https://doi.org/10.3389/fmicb.2018.00797>, 2018
- 599 Lindell, D., Erdner, D., Marie, D., Prasil, O., Koblizek, M., Le Gall, F., Rippka, R., Partensky, F., Scanlan, D.
600 J., and Post, A. F.: The nitrogen stress response of *Prochlorococcus* strain PCC 9511 (*Oxyphotobacteria*)
601 involves contrasting regulation of *ntcA* and *amt1*. *J. Phycol.*, 38, 1113-1124,
602 <https://doi.org/10.1046/j.1529-8817.2002.01205.x>, 2002.
- 603 Liu, H. B., Chang, J., Tseng, C. M., Wen, L. S., and Liu, K. K. Seasonal variability of picoplankton in the
604 northern South China Sea at the SEATS station. *Deep Sea Res. Part II Top Stud. Oceanogr.*, 54,
605 1602-1616, <https://doi.org/10.1016/j.dsr2.2007.05.004>, 2007.
- 606 Liu, Z., and Gan, J.: Open boundary conditions for tidally and subtidally forced circulation in a limited-area
607 coastal model using the Regional Ocean Modeling System (ROMS). *J. Geophys. Res.: Oceans*, 121,



- 608 6184-6203, <https://doi.org/10.1002/2016JC011975>, 2016.
- 609 Livak, K. J., and Schmittgen, T. D.: Analysis of relative gene expression data using real-time quantitative
610 PCR and the $2^{-\Delta\Delta CT}$ Method. *Methods*, 25, 402-408, <https://doi.org/10.1006/meth.2001.1262>, 2001.
- 611 Moore, L. R., Goericke, R. E., and Chisholm, S. W.: Utilization of different nitrogen sources by the marine
612 cyanobacteria, *Prochlorococcus* and *Synechococcus*. *Limnol. Oceanogr.* 47, 989-996,
613 <https://doi.org/10.4319/lo.2002.47.4.0989>, 2002.
- 614 Okabe, O., Tto, T., and Satoh, H.: (2003) Sulfate-reducing bacterial community structure and their
615 contribution to carbon mineralization in a wastewater biofilm growing under microaerophilic conditions.
616 *Appl. Microbiol. Biotechnol.*, 63, 322-334, <https://doi.org/10.1007/s00253-003-1395-3>, 2003.
- 617 Pedros-Alio, C.: Marine microbial diversity: can it be determined? *Trends. Microbiol.*, 14, 257-263,
618 <https://doi.org/10.1016/j.tim.2006.04.007>, 2006.
- 619 Qin, W., Amin, S. A., Martens-Habbena, W., Walker, C. B., Urakawa, H., Devol, A. H., Ingalls, A. E.,
620 Moffett, J. W., Armbrust, E. V., and Stahl, D. A.: Marine ammonia-oxidizing archaeal isolates display
621 obligate mixotrophy and wide ecotypic variation. *Proc. Natl. Acad. Sci. USA*, 111, 12504-12509,
622 <https://doi.org/10.1073/pnas.1324115111>, 2014.
- 623 Rusch, D. B., Martiny, A. C., Dupont, C. L., Halpern, A. L., and Venter, J. C.: Characterization of
624 *Prochlorococcus* clades from iron-depleted oceanic regions. *Proc. Natl. Acad. Sci. USA*, 107,
625 16184-16189, <https://doi.org/10.1073/pnas.1009513107>, 2010.
- 626 Shaw, P., and Chao, S.: (1994) Surface circulation in the South China Sea. *Deep-Sea Res. Part I*, 41,
627 1663-1683, [https://doi.org/10.1016/0967-0637\(94\)90067-1](https://doi.org/10.1016/0967-0637(94)90067-1), 1994.
- 628 Soliman, T., Reimer, J. D., Yang, S. Y., Briones, A. V., Roy, M. C., and Kodama, H. J.: Diversity of
629 microbial communities and quantitative chemodiversity in layers of marine sediment cores from a
630 causeway (Kaichu-Doro) in Okinawa Island, Japan. *Front. Microbiol.*, 11, 2451,
631 <https://doi.org/10.3389/fmicb.2017.02451>, 2017.
- 632 Stevens, H., and Ulloa, O.: Bacterial diversity in the oxygen minimum zone of the eastern tropical South
633 Pacific. *Environ. Microbiol.*, 10, 1244-1259, <https://doi.org/10.1111/j.1462-2920.2007.01539.x>, 2008.
- 634 Teixeira, L. M., and Merquior, V. L. C.: The family Moraxellaceae, *The Prokaryotes*, 443-476, 2014.
- 635 Török, I., and Kondorosi, A.: Nucleotide sequence of the *R. meliloti* nitrogenase reductase (*nifH*) gene.
636 *Nucleic Acids Res.*, 9, 5711-5723, 1981.
- 637 Tseng, C. H., Chiang, P. W., Lai, H. C., Shiah, F. K., Hsu, T. C., Chen, Y. L., Wen, L. S., Tseng, C. M., Shieh,
638 W. Y., Saeed, I., Halgamuge, S., and Tang, S. L.: Prokaryotic assemblages and metagenomes in pelagic
639 zones of the South China Sea. *BMC Genomics*, 16, 219, <https://doi.org/10.1186/s12864-015-1434-3>,
640 2015.



- 641 Venter, J. C., Reminton, K., Heidelberg, J. G., Halpern, A. L., Rusch, D., Eisen, J. A., Wu, D., Paulsen, I.,
642 Nelson, K. E., Nelson, W., Fouts, D. E., Levy, S., Knap, A. H., Lomas, M. W., Nealson, K., White, O.,
643 Peterson, J., Hoffman, J., Parsons, R., Baden-Tillson, H., Pfannkoch, C., Rogers, Y. H., and Smith, H. O.:
644 Environmental genome shotgun sequencing of the Sargasso Sea. *Science*, 304, 66-74,
645 <https://doi.org/10.1126/science.1093857>, 2004.
- 646 Voss, M., Bombar, D., Natalie, L., and Dippner, J. W.: Riverine influence on nitrogen fixation in the
647 upwelling region off Vietnam, South China Sea. *Geophys. Res. Lett.*, 33, L07604,
648 <https://doi.org/10.1029/2005GL025569>, 2006.
- 649 Wu, J. F., Chung, S. W., Wen, L. S., Liu, K. K., Chen, Y. L. L., Chen, H. Y., and Karl, D. M.: Dissolved
650 inorganic phosphorus, dissolved iron, and Trichodesmium in the oligotrophic South China Sea. *Global*
651 *Biogeochem. Cycles*, 17, 1008, <https://doi.org/10.1029/2002GB001924>, 2003.
- 652 Wu, C., Fu, F. X., Sun, J., Thangaraj, S. and Pujari, L.: Nitrogen fixation by Trichodesmium and unicellular
653 diazotrophs in the northern South China Sea and the Kuroshio in summer. *Sci. Rep.*, 8, 2415,
654 <https://doi.org/10.1038/s41598-018-20743-0>, 2018.
- 655 Xia, X. M., Guo, W., and Liu, H. B.: Dynamics of the bacterial and archaeal communities in the northern
656 South China Sea revealed by 454 pyrosequencing of the 16S rRNA gene. *Deep Sea Res. Part II: Top. Stud.*
657 *Oceanogr.*, 117, 97-107, <https://doi.org/10.1016/j.dsr2.2015.05.016>, 2015.
- 658 Xiao, P., Jiang, Y. G., Liu, Y., Tan, W. H., Li, W. H., and Li, R. H.: Re-evaluation of the diversity and
659 distribution of diazotrophs in the South China Sea by pyrosequencing the *nifH* gene. *Mar. and Freshwater*
660 *Res.*, 66, 681-691, <https://doi.org/10.1071/MF14134>, 2015.
- 661 Xiao, W. P., Wang, L., Laws, E. A., Xie, Y. Y., Chen, J. C., Liu, X., Huang, B. Q.: Realized niches explain
662 spatial gradients in seasonal abundance of phytoplankton groups in the South China Sea. *Prog.*
663 *Oceanogr.*, 162, 223-239, <https://doi.org/10.1016/j.pocean.2018.03.008>, 2018.
- 664 Xie, Y. Y., Laws, E. A., Yang, L., Huang, B. Q.: Diel patterns of variable fluorescence and carbon fixation of
665 picocyanobacteria *Prochlorococcus*-dominated phytoplankton in the South China Sea Basin. *Front.*
666 *Microbiol.*, 9, 1589, <https://doi.org/10.3389/fmicb.2018.01589>, 2018.
- 667 Yu, Y., Lee, C., Kim, J., and Hwang, S.: Group-specific primer and probe sets to detect methanogenic
668 communities using quantitative real-time polymerase chain reaction. *Biotechnol. Bioeng.*, 89, 670-679,
669 <https://doi.org/10.1002/bit.20347>, 2005.
- 670 Zehr, J. P., Crumbliss, L. L., Church, M. J., Omoregie, E. O., and Jenkins, B. D.: Nitrogenase genes in PCR
671 and RT-PCR reagents: implications for studies of diversity of functional genes. *Bio. Techniques*, 35,
672 996-1002, <https://doi.org/10.2144/03355st08>, 2003.
- 673 Zehr, J. P., Robidart, J., and Scholin, C.: Global environmental change demands a deeper understanding of



- 674 how marine microbes drive global ecosystems. *Microbe*, 6, 169-175, 2011.
- 675 Zhang, Y., Sintes, E., Chen, M. N., Zhang, Y., Dai, M. H., Jiao, N. Z., Herndl, G. J.: Role of mesoscale
676 cyclonic eddies in the distribution and activity of Archaea and Bacteria in the South China Sea. *Aquat*
677 *Microb Ecol* 56: 65-79, <https://doi.org/10.3354/ame01324>, 2009.
- 678 Zhang, Y., Zhao, Z. H., Dai, M. H., Jiao, N. Z., and Herndl, G. J.: Drivers shaping the diversity and
679 biogeography of total and active bacterial communities in the South China Sea. *Mol. Ecol.*, 23, 2260-2274,
680 <https://doi.org/10.1111/mec.12739>, 2014.
- 681 Zwart, G., Crump, B. C., Agterveld, M. P. K. V., Hagen, F., and Han, S. K.: Typical freshwater bacteria: an
682 analysis of available 16S rRNA gene sequences from plankton of lakes and rivers. *Aquat. Microb. Ecol.*,
683 28, 141-155, <https://doi.org/10.3354/ame028141>, 2002.
- 684 Zwirgmaier, K., Jardillier, L., Ostrowski, M., Mazard, S., Garczarek, L., Vaulot, D., Not, F., Massana, R.,
685 Ulloa, O., and Scanlan, D. J.: Global phylogeography of marine *Synechococcus* and *Prochlorococcus*
686 reveals a distinct partitioning of lineages among oceanic biomes. *Environ. Microbial.* 10, 147-161,
687 <https://doi.org/10.1111/j.1462-2920.2007.01440.x>, 2007.



Tables

Table 1 Sampling sites and physicochemical parameters.

Stations	Depth	Latitude (°N)	Longitude (°E)	Temperature (°C)	Salinity (PSU)	Chl a (mg/m ³)	DO	NO ₂ ⁻	NO ₃ ⁻	PO ₄ ³⁻	SiO ₃ ²⁻
SEATS	4m	18.00	116.00	29.81	33.69	0.116	5.79	BTD	BTD	BTD	1.67
	68m			22.57	34.57	0.899	6.65	BTD	0.25	BTD	2.74
	200m			14.18	34.53	0.004	4.8	BTD	17.56	1.20	25.77
	750m			5.90	34.47	0.026	2.75	BTD	35.98	2.62	104.33
SS1	4m	14.00	116.00	30.23	33.34	0.158	6.13	BTD	BTD	BTD	2.00
	105m			22.29	34.53	0.623	5.28	0.05	3.17	0.42	6.82
	200m			14.85	34.54	0.013	4.052	BTD	16.45	1.08	20.21
A2	6m	12.00	116.00	6.10	34.46	0.044	2.57	BTD	34.78	2.62	105.32
	750m			30.13	33.44	0.258	6.06	BTD	BTD	BTD	1.96
B1	6m	14.00	113.00	29.97	33.54	0.084	6.13	BTD	BTD	BTD	2.10
C1	4m	12.00	113.00	29.96	33.40	0.139	6.09	BTD	BTD	BTD	2.13

PSU, practical salinity unit; Chla, chlorophyll a. “BTD” means the value is below the detection limit. The upper measuring limits of the AA3 Analyzer as referred to NO₂⁻, NO₃⁻, PO₄³⁻ and SiO₃²⁻ are 0.04 μM, 0.1 μM, 0.08 μM and 0.16 μM, respectively.



Table 2 The spearman's correlations between bacterial and diazotrophic community, and environmental factors.

	Spearman's correlation							
	T	Salinity	Chl a.	NO ₂ ⁻	NO ₃ ⁻	PO ₄ ³⁻	SiO ₃ ²⁻	DO
Bacterial diversity								
OTUs	-0.518	0.200	-0.700*	-0.100	0.648*	0.778**	0.591	-0.793**
Ace	-0.445	0.077	-0.773**	-0.300	0.563	0.689*	0.573	-0.692*
Shannon index	-0.327	0.465	-0.273	0.100	0.181	0.243	0.200	-0.323
PCoA axis I	-0.0909**	0.761**	-0.600	0.000	0.915**	0.843**	0.800**	-0.692*
Bacterial structure								
Bray-Curtis distance	0.7974**	0.2829*	0.092	-0.154	0.7653**	0.700**	0.737**	0.673**
Diazotrophic diversity								
OTUs	0.394	-0.565	-0.333	-0.522	-0.200	-0.089	-0.079	0.225
Ace	0.697*	-0.863**	-0.176	-0.522	-0.627	-0.464	-0.491	0.413
Shannon index	-0.079	-0.316	-0.285	-0.290	0.162	0.225	0.333	-0.061
PCoA axis I	-0.685*	0.766**	-0.127	0.406	0.769**	0.676*	0.648*	-0.529
Diazotrophic structure								
Bray-Curtis distance	0.564*	0.227	0.219	0.265	0.545*	0.519*	0.542*	0.505*

**P < 0.01 and *P < 0.05 indicate significant correlation.



Figure legends

Figure 1. Sampling sites of the South China Sea basin

Figure 2. Differences in bacterial and diazotrophic community richness, diversity and structure from horizontal and vertical bacterial samples in the Northern and Southern SCS: (a, b) The richness of the bacterial community and the diazotrophic community; (c, d) The diversity of the bacterial community and the diazotrophic community; (e, f) Principal Coordinate Analysis (PCoA) of the bacterial community and the diazotrophic community; (g, h) Hierarchical clustering tree on 16s rRNA OTU level and on nifH OTU level.

Figure 3. Relative abundances of bacterial and diazotrophic compositions of the nSCS and sSCS basin at phylum level: (a-b) Horizontal and vertical bacterial composition; (c-d) Horizontal and vertical diazotrophic composition; (e-f) Taxonomic groups of *Proteobacteria* in bacterial and diazotrophic community. *unclassified.

Figure 4. Relative abundances of the 10 most abundant OTUs at the family level in the horizontal and vertical bacterial samples of the nSCS and sSCS basin. *unclassified. *Gammaproteo* represents *Gammaproteobacteria*; *Pseudoalter* represents *Pseudoalteromonadaceae*; *Sphingomon* represents *Sphingomonadaceae*; *Salinispha* represents *Salinisphaeraceae*.

Figure 5. Top ten most abundant depth-specific OTU groups of the bacterial (a, b) and diazotrophic communities (c, d) from vertical nifH samples in the nSCS and sSCS basin. The area of each bubble represents the cumulative relative abundance in the sample examined; *unclassified.

Figure 6. Relative abundance of the 10 most abundant OTUs at the family level in the horizontal and vertical nifH samples of the nSCS and sSCS basin. *unclassified.

Figure 7. Horizontal (a) and vertical (b) distributions of N utilization genes predicted according to the bacterial OTUs in the nSCS and sSCS basin.

Figure 8. Relative transcripts of N utilization genes and relative transcripts of *amt1*, *urtA* and *AAT* in *Prochlorococcus* among different surface samples. Error bars represent the standard deviations of the values generated from three biological repeats.



Figure 1

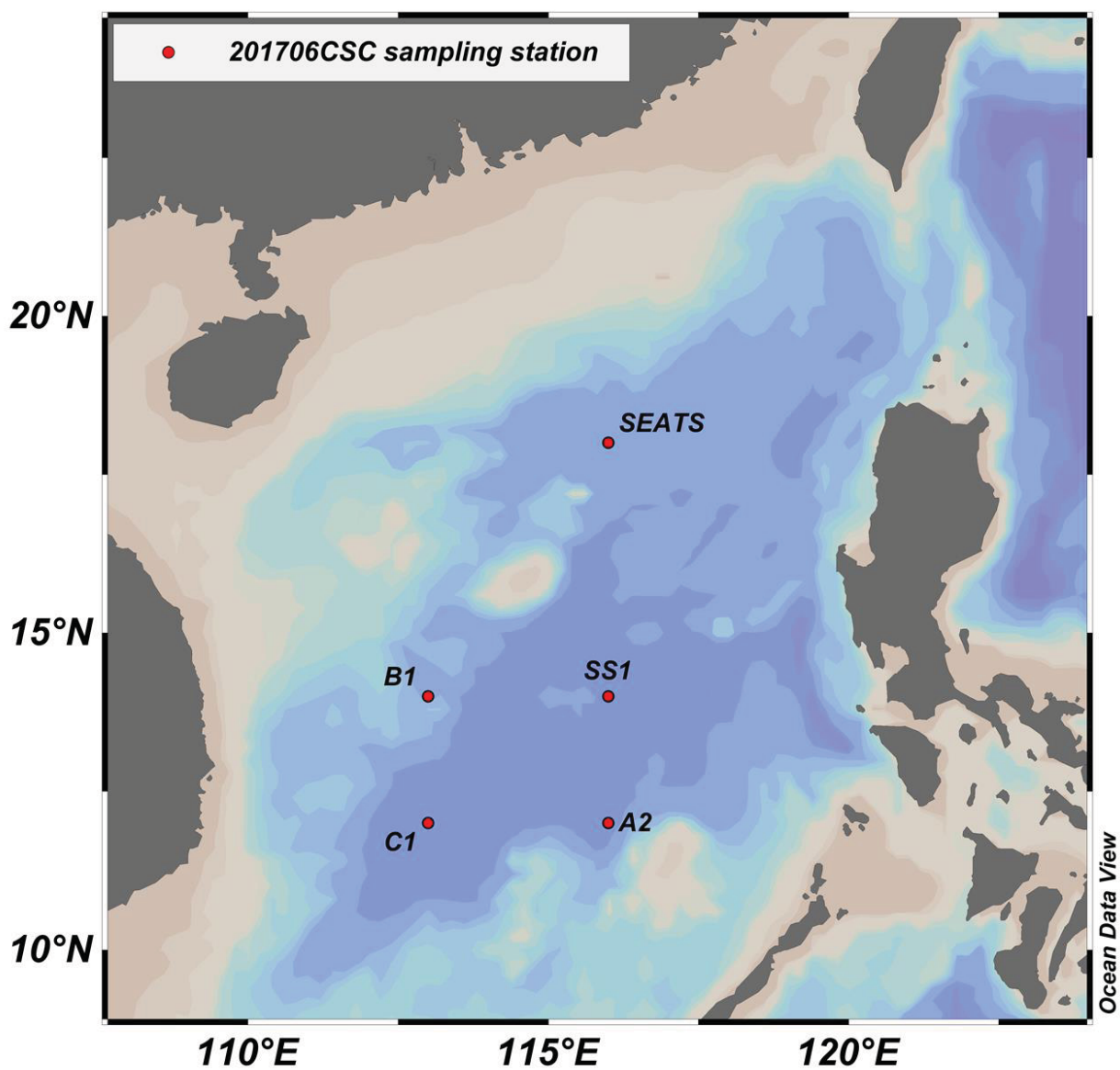




Figure 2

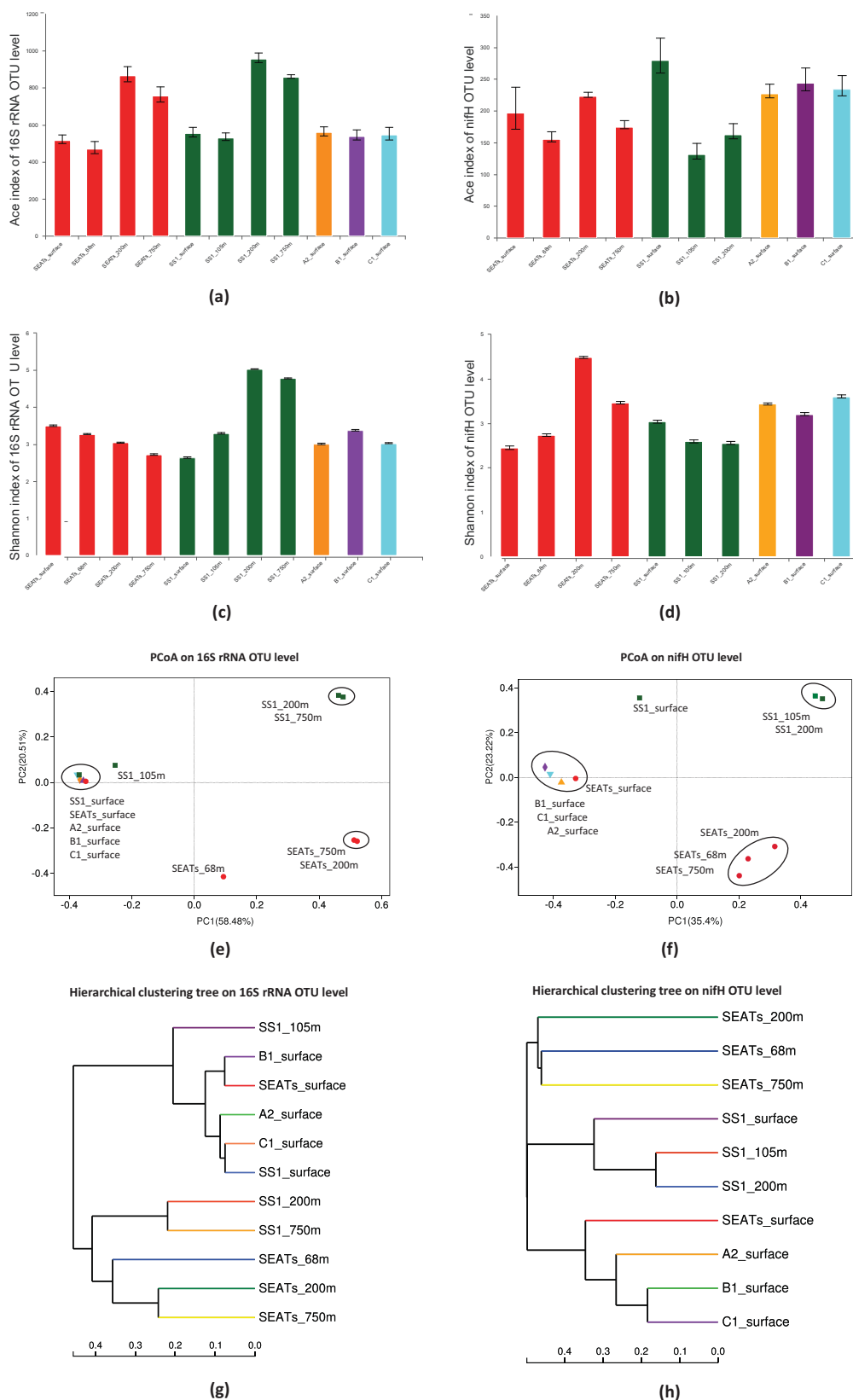




Figure 3

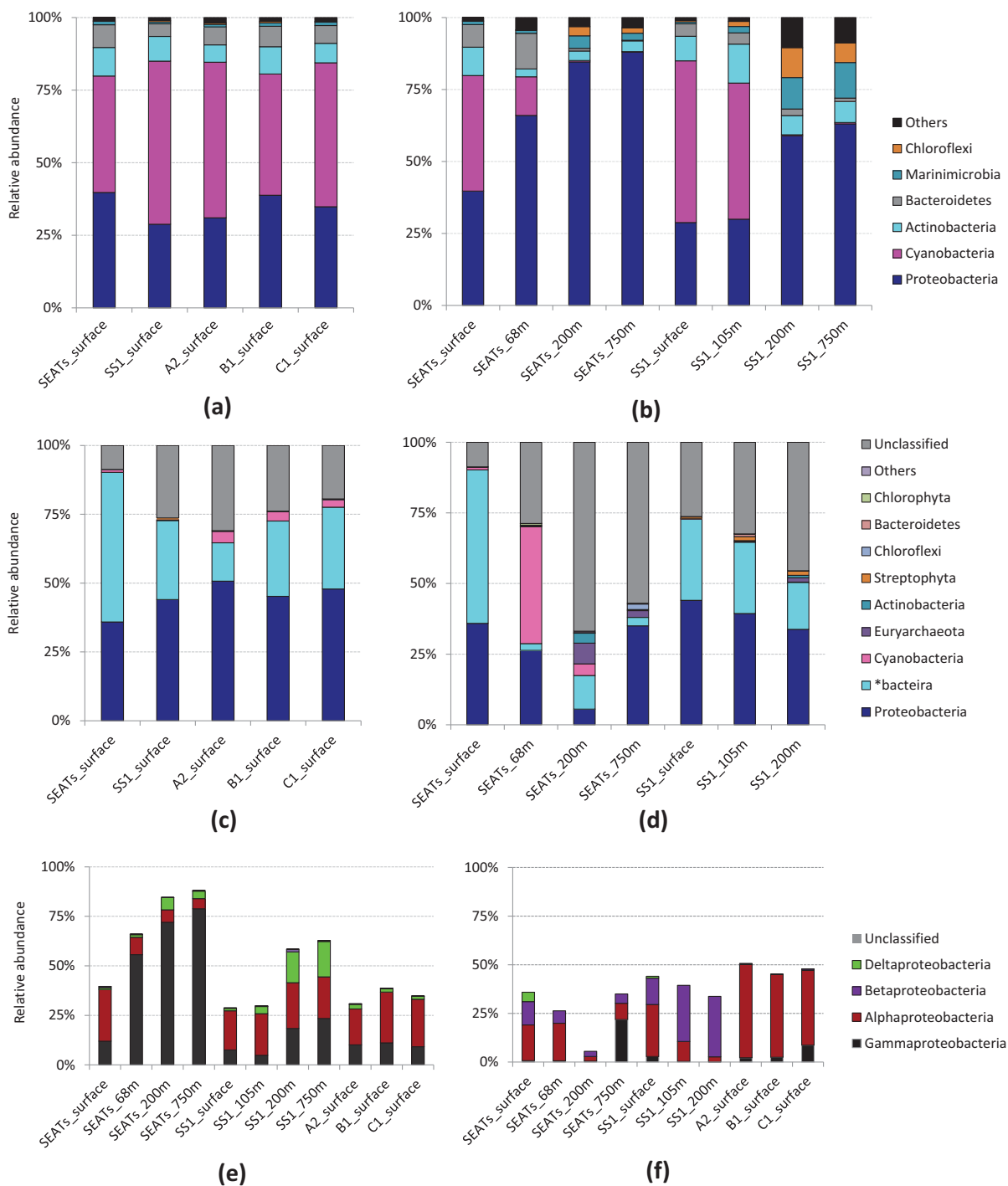




Figure 5

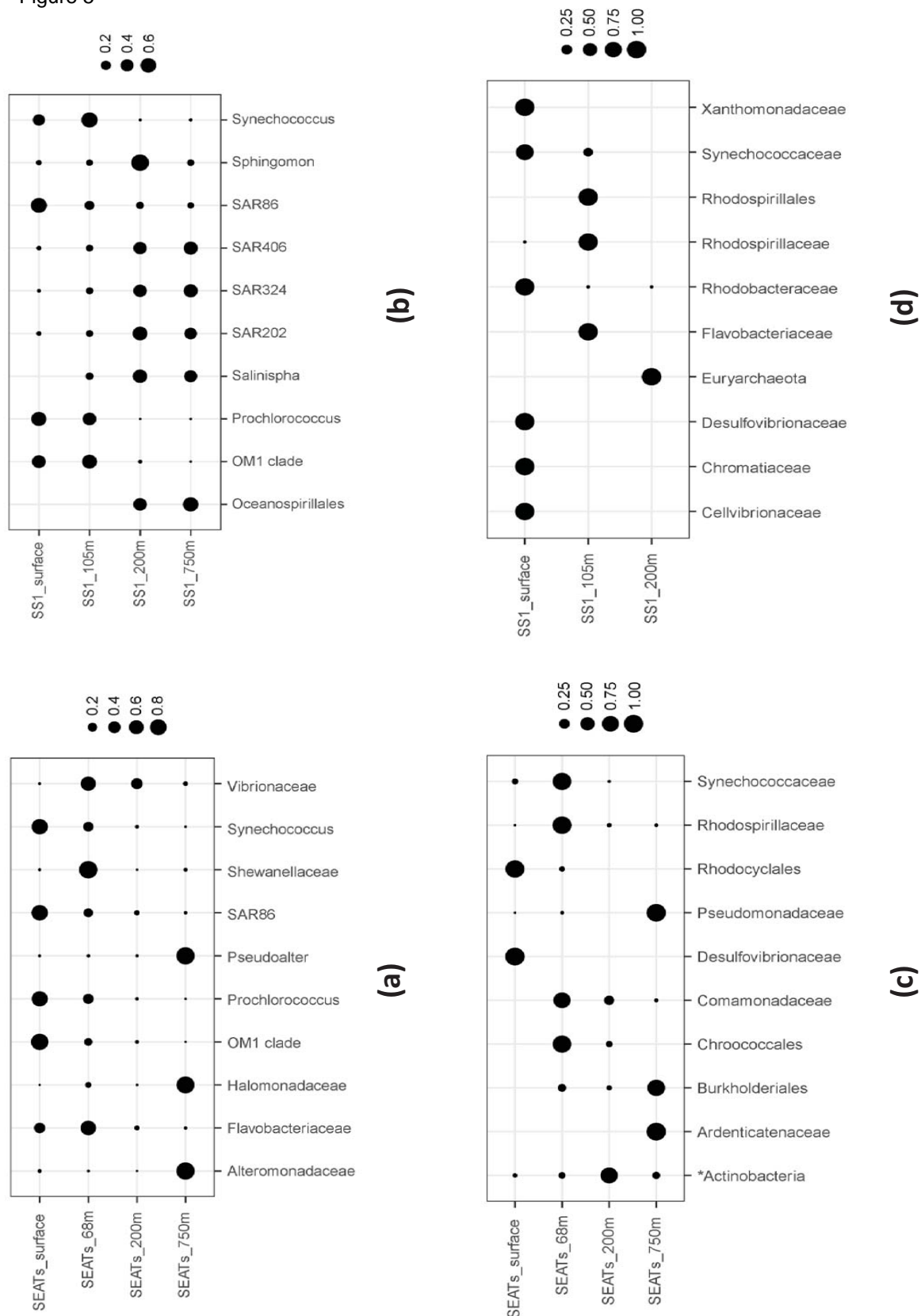




Figure 6

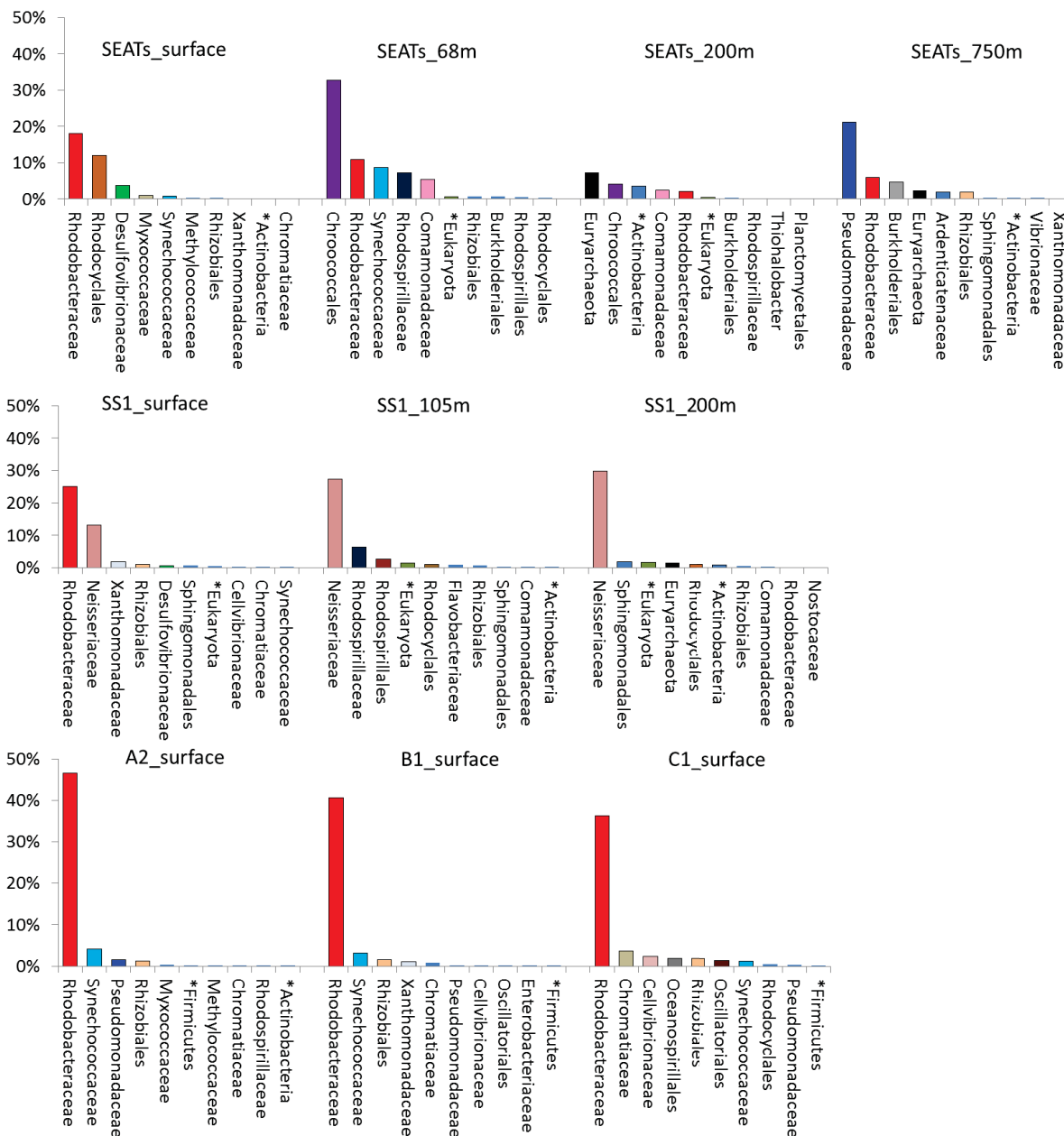
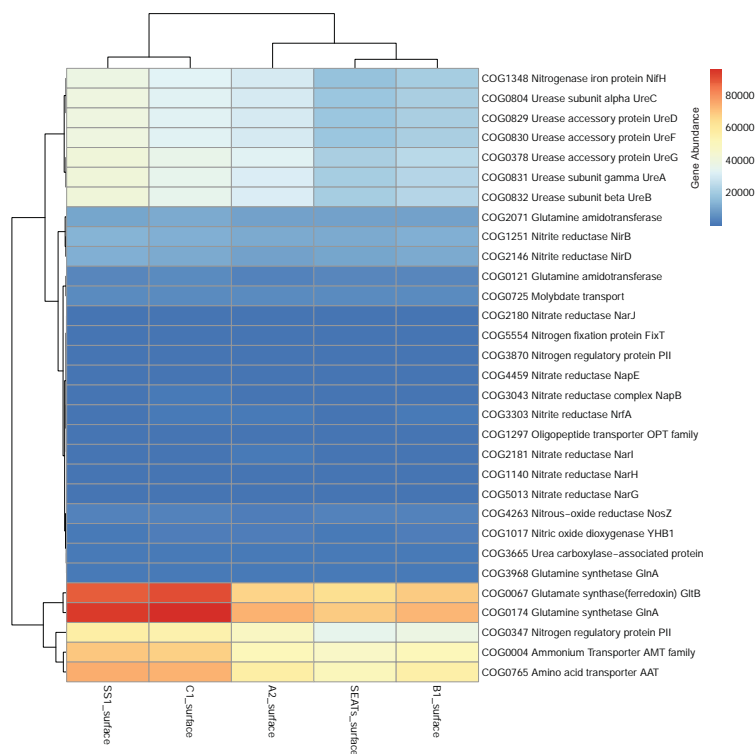
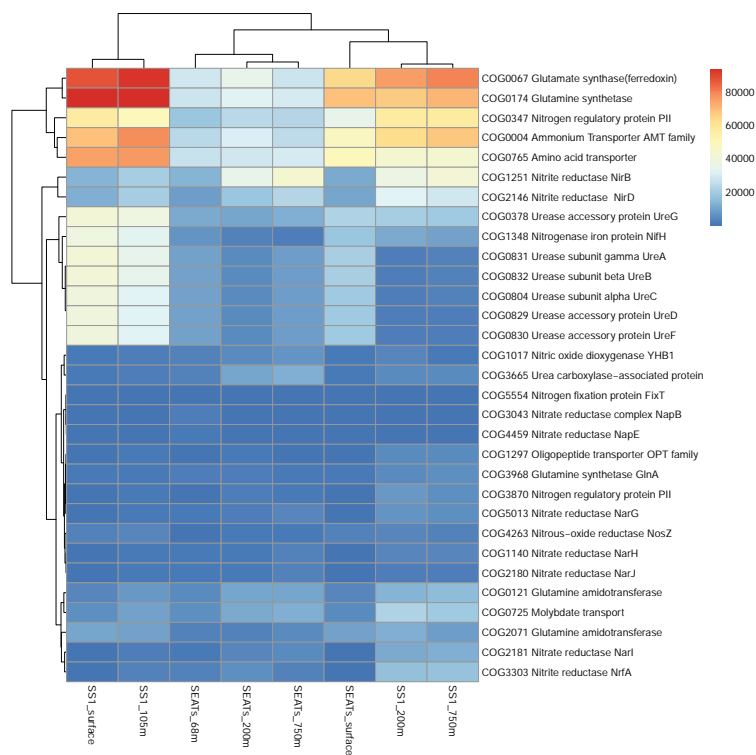




Figure 7



(a)



(b)



Figure 8

